Advances in Aircraft and Spacecraft Science, *Vol. 5, No. 2 (2018) 205-223*
DOI: https://doi.org/10.12989/aas.2018.5.2.205

Modelling and simulation of a closed-loop electrodynamic shaker and test structure model for spacecraft vibration testing

Steffen Waimer*[1,3], Simone Manzato[1], Bart Peeters[1], Mark Wagner[2] and Patrick Guillaume[3]

[1]*Siemens Industry Software NV, Researchpark 1237, 3001 Leuven, Belgium*
[2]*European Space Agency ESA/ESTEC, Keplerlaan 1, 2200 AG Noordwijk, The Netherlands*
[3]*Acoustics and Vibration Research Group, Vrije Universiteit Brussel, Pleinlaan 2, 1050 Brussels, Belgium*

(Received November 28, 2016, Revised September 13, 2017, Accepted October 12, 2017)

Abstract. During launch a spacecraft is subjected to a variety of dynamical loads transmitted through the launcher to spacecraft interface or air-born transmission excitations in the acoustic pressure field inside the fairing. As a result, spacecraft are tested on ground to ensure and demonstrate the global integrity of the structure against these loads, to screen the flight hardware for quality of workmanship and to validate mathematical models. This paper addresses the numerical modelling and simulation of the low frequency sine and random vibration tests performed on electrodynamic shaker facilities to comprise the mechanical-borne transmission loads through the launcher to spacecraft interface. Consequently, the paper reviews techniques and methodologies to derive a reliable and representative coupled virtual vibration testing simulation environment based on experimental data. These technologies are explored with the main objectives to ensure a stable, reliable and accurate control while testing. As a result, the use of the derived simulation models in combination with the added value of improved control and signal processing algorithms can lead to a safer and smoother vibration test control of the entire environmental test campaign.

Keywords: environmental spacecraft testing; multiphysics modelling and simulation; experimental system identification; structural coupling; vibration control

1. Introduction

In spacecraft (S/C) engineering, environmental testing is a crucial part to ensure and demonstrate the spacecraft's integrity against the dynamical launch environment, to screen the flight hardware for quality of workmanship and to validate mathematical models, NASA (2014). Hence, vibration testing is performed on big electrodynamic or hydraulic shaker testing facilities which are often one of its kind test setups, e.g., the six degree-of-freedom (DoF) hydraulic shaker HYDRA at the European Space Research and Technology Centre (ESTEC) in Noordwijk or multiple electrodynamic shaker configurations for vibration testing of large S/C in lateral and vertical directions as reported by ECSS (2013), Appolloni and Cozzani (2007) and Appolloni *et al.* (2015). Those test campaigns are a mandatory part in the S/C development process to qualify the

*Corresponding author, E-mail: steffen.waimer@siemens.com

Copyright © 2018 Techno-Press, Ltd.
http://www.techno-press.org/?journal=aas&subpage=7 ISSN: 2287-528X (Print), 2287-5271 (Online)

mechanical designed S/C structure for launch as defined in the 'Spacecraft mechanical loads analysis handbook' of the European Cooperation for Space Standardisation, ECSS (2013), to experimentally simulate the low frequency structural and mechanical-borne transmission loads through the launcher-spacecraft interface to the test specimen.

While testing, especially of large S/C with misalignments in the Centre-of-Gravity (CoG) between the testing facility and test specimen, the interaction between the structure under test, the vibration controller and the hardware used to perform the test is a critical issue. The dynamics of the testing facility often couples with that of the test specimen at some specific frequency ranges. This can lead to violation of test specifications and undesired challenges while testing, e.g., beating phenomena which usually occur in a frequency range close to structural resonances, and can result in over- or under testing, or even damage of the S/C as concerned in different publications especially by ECSS (2013), Bettacchioli (2014), and Bettacchioli and Nali (2015). A solution to these problems and limitations can be achieved by simulating the test in advance to its physical execution which is often called virtual (shaker) testing at first mentioned in this context by Appolloni and Cozzani (2007). The main objective is to predict the outcome of the vibration test numerically to optimise control parameter and to apply notching strategies to tackle these issues. Therefore, the simulation environment needs to comprise the main contributors of the vibration test chain:

- the S/C or structure being tested including all test brackets and adapters,
- the excitation system (electrodynamic or hydraulic vibration system) and
- the vibration control system active during test.

An important part of this environment is the shaker generating the vibrations, but in practice, a detailed and validated electrodynamic numerical simulation model of a shaker is not readily available.

Therefore, the first part of the paper reviews the derived enhanced shaker model based on a tailored experimental system identification methodology. Extensive simulation studies are performed to validate the multiphysical vibration system, to virtually replicate sine control tests and to anticipate possible difficulties or violations of test specifications, e.g., the occurrence of beating phenomena at lightly damped shaker resonances.

The second part of the paper focuses on the experimental derivation of specific structural models, e.g., coupled Head Expander (HE) and test specimen model and the dynamical coupling to a closed-loop electrodynamic shaker and sine controller model in the future.

Accordingly, the gained physical and dynamical system insight in combination with system identification knowledge from modelling, simulation and testing is applied to improve the entire vibration test and control performance i.e., pre-shaping of shaker drives by considering inverse system transfer functions and pre-defined test specifications, and adjusting of control parameter.

More specifically, the first part of this paper introduces in Sec. 2 the current status of work to derive the virtual shaker simulation environment. In detail, Sec. 2.1 summarises the work which has been performed to derive and implement an enhanced five DoF electrodynamic shaker model based and continuing the work of previous publications of Lang and Snyder (2001), Ricci *et al.* (2009) and Manzato *et al.* (2014). In Sec. 2.2, a numerical simulation study on the enhanced shaker model is presented to evaluate the occurrence of beating phenomena influenced by different control parameter settings. Subsequently, a first step for the dynamical coupling of test structures is investigated by performing modal analysis of the shaker HE and a beam test structure in Sec. 3. The experimental hammer impact test results of both structures alone and in coupled configuration in free-free boundary conditions are presented and analysed to determine an experimental data set

as basis to apply dynamical substructuring techniques in the frequency and modal domain in the future. The main goal of this study which is still under research is the investigation and evaluation of preliminary coupling techniques and guidelines to comprise coupled dynamical structural test specimen models and the electrodynamic shaker model in further numerical simulations. Sec. 4 uses the estimated experimental findings to apply a test data driven first modelling methodology for numerical sine control test predictions. Consequently, the calculated results are partially evaluated against real physical test data in a qualitative manner.

Finally, a preliminary study is performed to improve the entire vibration test and control performance by directly applying the gathered dynamic system information in a pre-shaping architecture to modify the shaker drives. These analysis and results are presented in Sec. 5 and are used to highlight the possibility of using test data from the system self-check prior to the sine control execution for control enhancement.

2. Virtual shaker simulation environment

2.1 Review of electrodynamic shaker and sine controller model

This section gives an overview of the derivation of a coupled shaker to vibration controller model which defines a crucial part of the virtual simulation environment. A principle sketch is shown in Fig. 1.

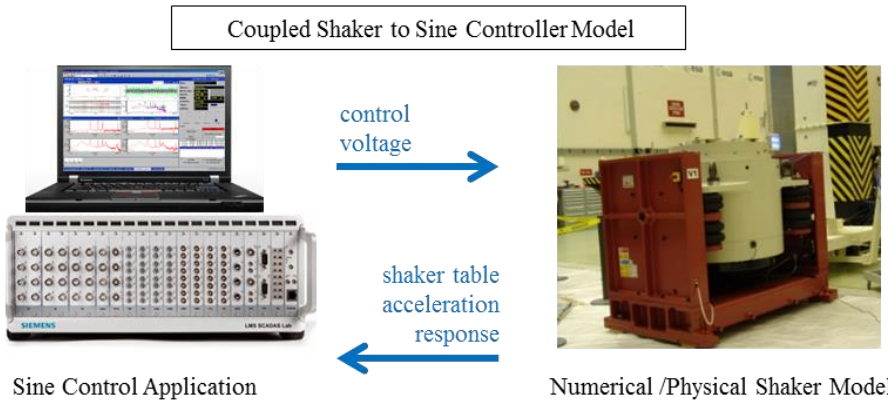

Fig. 1 Sketch of the LMS Test.Lab sine control model coupled to the numerical model of ESTEC's 160 kN shaker. The control voltage and shaker table acceleration close the vibration control loop. Picture courtesy Siemens Industry Software NV and European Space Agency (ESA)

The shaker facility (in the right part of Fig. 1) interacts with the vibration test controller (in the left part of Fig. 1) by a closed-loop acceleration feedback control system to be capable of controlling the shaker table acceleration with reference to required test specifications. Due to its large number of installations at vibration space testing centres, LMS Test.Lab Sine Control is implemented and used to conduct controlled virtual sine sweep tests. The sine controller model has been derived and extensively validated to the existing hardware and software implementation of

Siemens Industry Software NV (2016a, b) as reported in previous works by Ricci *et al.* (2009) and Manzato *et al.* (2014). An important part of this environment is the shaker generating the vibrations, but in practice, a detailed and validated electrodynamic numerical simulation model of a shaker is not readily available. Hence, a lumped-parameter shaker model according to Lang and Snyder (2001) is implemented in Matlab/Simulink. It represents a common and simplified electromechanical model valid under a large variety of numerical shaker models and constitutes one crucial part for virtual shaker testing. It is intended that the modelling approach considers experimental system identification data to derive and update model parameters and to improve the entire dynamic system performance.

The left sketch in Fig. 2 shows the principle mechanical and electrical parts of such a lumped-parameter, one-dimensional, three DoFs, electromechanical shaker model as introduced by Lang and Snyder (2001) and further applied in the field of virtual shaker testing by Ricci *et al.* (2009), Manzato *et al.* (2012) and Waimer *et al.* (2015) in previous research activities. In principle it describes a basic model of a modal shaker. The assembly of coil and table is often called armature and represents the moving elements of the electrodynamic shaker. The compliant connection between the armature assembly and the body forms a mass, spring and damper system defining a single DoF system. Adding two more DoFs completes the mechanical model: firstly, the armature structure is modelled as being elastic and not rigid by treating the coil and table as separate masses, connected by a spring and damper system, and secondly, the isolation system of the shaker to the ground is modelled with a second spring and damper system. When an electrical current i is conducted through the coil, an axial force, according to the electromagnetic Lorentz force, is produced and transmitted through the suspension system to the table structure resulting in a vertical motion.

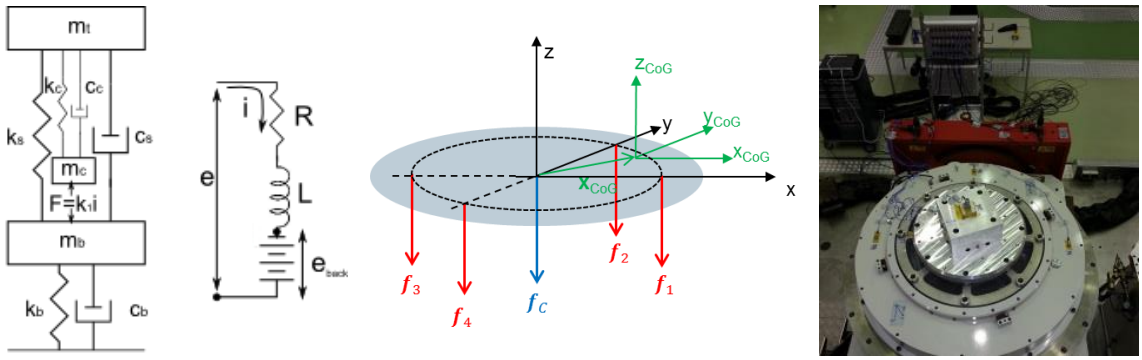

Fig. 2 On the left, sketch of the lumped parameter electrodynamic shaker model, Lang and Snyder (2001). In the centre, modifications on the shaker table to add rotational shaker table dynamics, Waimer *et al.* (2016a). On the right, top view to ESTEC's 160 kN shaker with sensor instrumentation and test masses for system identification, picture courtesy ESA

The system identification is applied to real test data gathered at the system identification test campaign using the 160 kN shaker at ESTEC. The results are summarised in Waimer *et al.* (2015) using a global approach and a combination of sine and random control data to enhance the quality of the estimated parameter of the entire frequency band up to 2000 Hz. In this case, the experimental results of the first two loading configurations (Empty shaker table and Interface disc)

are applied to determine the shaker parameters and used to predict the test performance of the third loading configuration (Interface disc and cuboid) as shown by the right picture of Fig. 2. Test and simulation results are shown by the acceleration-over-electrical current frequency response functions (FRF) in the left part of Fig. 3. The plot shows the system dynamics of ESTEC's 160 kN shaker facility calculated from a sine control simulation considering the Interface disc and cuboid (measured in blue and predicted in dashed green) and Interface disc and HE (measured in black and predicted in dashed red) loading configuration. The numerical predictions are calculated by using the three DoF shaker model and the global parameter approach. It is confirmed that the major system characteristic such as suspension and coil mode can be predicted for both cases. But for the Interface disc as well as the HE configuration, an additional structural resonance occurs because of the flexibility of these components and, therefore, it cannot be anymore represented by a rigid lumped mass or ideal loading case. The latter assumption is removed in this paper, by focusing on the coupling of structural models in Sec. 3.

Summarizing, at the current status, the shaker table specifically consists of one translational DoF which is capable of representing the shaker's dynamical characteristic for the idealized test. For these cases the current shaker model can be used to recalculate and predict test results in open and closed-loop random and sine control operations as shown by the dashed green FRFs in Fig. 3. However, considering idealized and centered loading and sensor conditions some deviations occur between the test and simulation results. In practice, these deviations will increase, if complex test structures are attached to the shaker and idealized conditions cannot be applied anymore. Especially for S/C vibration testing, the CoG of the S/C and shaker table is rarely aligned to each other with reference to the main vertical axis of motion. As consequence, the entire system tends to be subjected to undesired rotational and lateral dynamical movements during test. A first main problem is the dynamical coupling between the first bending mode of the structure under test and the rocking (rotational) mode of the shaker table. This is a main reason, for virtual shaker testing and to follow a multi-domain modelling and simulation approach, including the test structure, excitation system and control system in order to assess the global performance, Appolloni and Cozzani (2007). To predict this, an enhanced shaker model with two additional rotational DoF has been derived. A principal sketch is presented in the centred picture of Fig. 2 assuming the suspension system to be spatially distributed, the Lorentz force acting on the centre without rotational dynamics and the rotation point to be equal to the CoG of the coupled system. More information is presented in Waimer *et al.* (2016a).

As a first application, the enhanced shaker model is implemented and verified against hammer impact results of the Interface disc and cuboid loading configuration as presented by the right plot of Fig. 3. Therefore, the hammer impacts are numerically approximated and simulated by defining an input moment M_{in} as excitation on the shaker table, similarly to the experimental conditions. The results show a good agreement between the experimental and numerical results, although some deviations are observable which will be investigated in more detail in the future. Additionally, the simulation model is used to show the dynamical differences if the shaker is switched off/on. The main differences are that the suspension mode is highly damped and it is only observable with the shaker turned off, the rocking modes are unchanged and the coil mode is slightly increased if the shaker is switched on as reported by McConnell and Varoto (1995).

2.2 Numerical simulation of beating phenomena and post processing analysis

The derived five DoF shaker model in sine control application is used to simulate possible

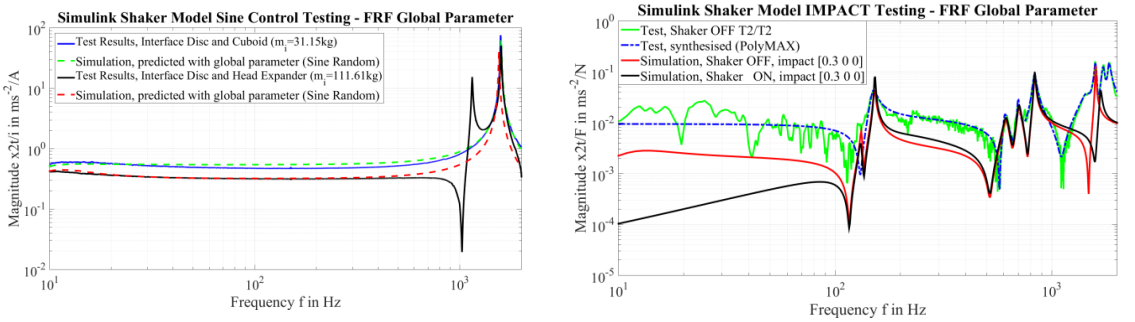

Fig. 3 160 kN shaker of ESTEC. On the left, correlation between experimental test results (Interface disc/cuboid in blue and Interface disc/Head Expander in black) and sine control simulations (dashed green and red lines) using the simplified shaker model applying the estimated global set of parameter. On the right, correlation between hammer impact excitation test results on impact location T2 (-x-axis) and simulated results with enhanced shaker model

challenges which usually occur during S/C vibration testing of large S/C with not negligible misalignments between CoGs. The most probable dynamic effects are beating phenomena influenced by the sine control sweep rate and compression factor applied during control. According to ECSS (2013) and industrial publications of Thales Alenia Space by Bettacchioli (2014), and Bettacchioli and Nali (2015), the most common issue is induced if the sweep rate is not sufficiently slow, then the dynamic and coupled system response is no longer stationary (steady-state) at each instant of time and spectral sine excitation which results in a modification of the time response envelop due to transient behaviour. The shape and position of a resonant peak, e.g. structural test specimen modes, rotational shaker table dynamics or a coupled S/C to shaker mode is altered as a function of the sweep rate and direction. Additionally, ringing effects may occur as a result of the system responding and interfering of two nearly spaced frequencies, comprising the free system response at the natural frequency and the forced response of the swept excitation. In industrial practice, sweep rate effects are not yet considered in currently applied base-driven finite element model (FEM) vibration simulations in hard mounted boundary conditions and can lead to misinterpretations of experimental results. Therefore, it will be a valuable asset to include the virtual shaker testing approach in the S/C vibration testing procedure.
The simulations shown in this section to analyze the beating phenomena focus only on the interaction between the rotational shaker table modes, as structural test specimen models are not yet part of the simulation environment. Hence, numerical sine control tests are executed on the five DoFs shaker model whereas the damping of the low frequency 1st rotational mode at approx. 130 Hz is decreased by a factor of 10 in comparison to the 2nd rotational mode at approx. 150 Hz to simulate the beating phenomena for two different sweep rates. Fig. 4 shows at the top left the calculated voltage, current and acceleration spectra for a fast-linear sweep rate of 10 Hz/s in blue and a slow linear sweep rate of 1 Hz/s in green, both in sweep up direction. The beating effect is clearly visible as deviation in the acceleration control spectra (green and blue) to the reference control spectra of 0.5 g in red. To give a clearer view about how the beating evolves with different sweep rates and directions the bottom plot highlights the evolution of the spectra w.r.t. diverse logarithmic sweep rates in both sweep directions. For both plots, the resonance shifts with sweep direction and the following ringing effect decreases with lower sweep rates resulting in a better vibration control. In practice, it is usually not possible to apply very low sweep rates to provide

better control in this way, since the risk of damaging the structure under test increases as well as the testing time. The right plots of Fig. 4 show the approximated time-frequency acceleration spectrum by applying the Wavelet transform with the Morlet wavelet to the simulated time data of the fast-linear sweep-up rate of +10 Hz/s at the top and the fast-logarithmic sweep-down rate of -12 oct/min at the bottom, respectively. It is calculated analogous to the Fourier transform as the convolution between the signal and the wavelet function, which is a short oscillating function containing both the trigonometric analysis function and the window. A major advantage is that it retrieves the time- frequency information by shifting the wavelet over the signal optimizing its resolution by adapting (contracting and dilating) the wavelet function, Merry and Steinbuch (2005), Mao (2016).

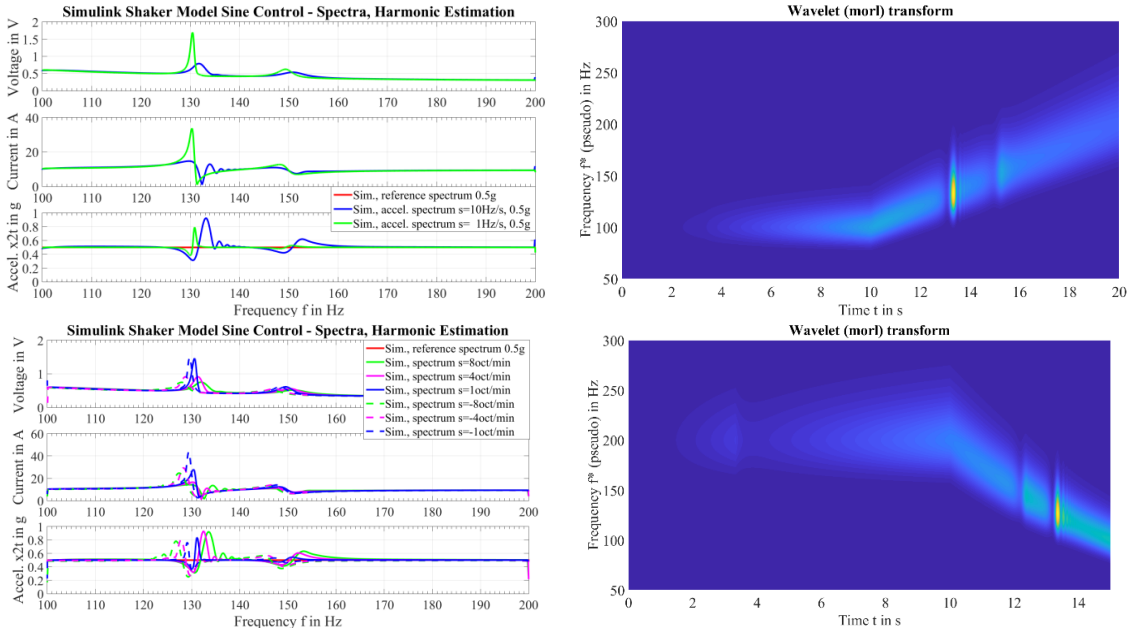

Fig. 4 On the left, spectra (voltage, current and shaker table acceleration) of the enhanced shaker table model coupled to the sine controller model to investigate numerically the occurrence of beating at rotational shaker table modes influenced by different linear and logarithmic sweep rates at the top and bottom, respectively. On the right, Wavelet transform as signal post-processing alternative to visualize sine control results of a linear sweep-up rate of +10 Hz/s at the top and a logarithmic sweep-down rate of -12 oct/min at the bottom

The plots of the Wavelet transformation show at first the build-up time of 10 s of the controller before the actual sine sweep starts and the excitation of the two rotational shaker table modes in sweep direction and rate. The sharp and lowly damped first mode is influenced by the beating and ringing phenomena similarly as seen by the spectra on the left plots of Fig. 4, whereas the second mode is less influenced by the beating and closer to the reference profile.

Additionally, to the sweep rate and its direction, the compression factor has also an influence on the control application and the beating phenomena. The compression factor is a parameter which needs to be specified to adapt the robustness and responsiveness of the control. In detail, it is used as a weighting factor in the control algorithm to minimize overshoots and to limit cross-

talks. In this case, the compression factor can take integer values between 1 and 20: a low compression factor leads to a faster control with an immediate correction of the control error, while a high value results in a more stable but slower control action, Ricci *et al.* (2009). In analogy to the previous study of the effect of the sweep rate summarized in Fig. 4, the same enhanced shaker model is used to investigate the influence of the compression factor. Therefore, Fig. 5 shows the numerical simulation results and consequently the effect of changing the compression factor (c=[8,6,4]) at two sweep rates of 1 oct/min on the left and 4 oct/min on the right, and its influence on the control performance. Analyzing the spectra, especially the acceleration spectra at the bottom, show that for a constant sweep rate a lower compression factor (c=4 in dotted black) results in a better control with smaller amplitude deviation from the reference control spectrum, a decreased frequency shift in the sweep direction and less broadening of the mode. However, it slightly increases the oscillations (ringing) after passing the resonance frequency of the mode. As result of this numerical study, it is summarized that both the sweep rate and the compression factor influence the occurrence of the beating phenomena whereas the effect of the sweep rate dominates it.

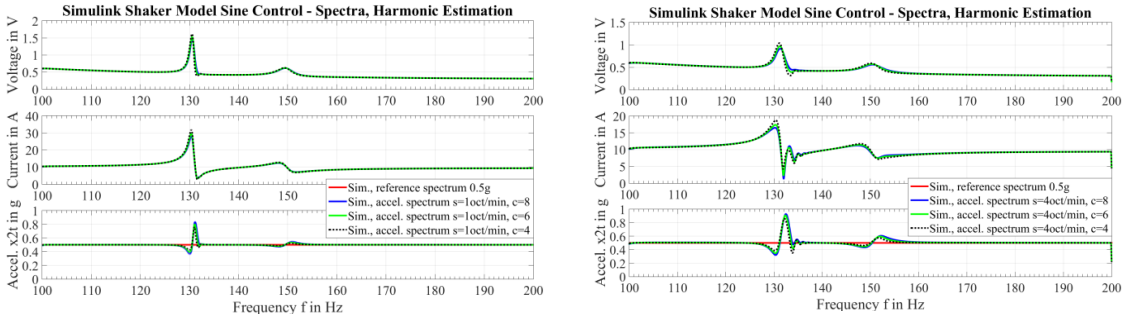

Fig. 5 Spectra (voltage, current and shaker table acceleration) of the enhanced shaker table model coupled to the sine controller model to investigate numerically the occurrence of beating at rotational shaker table modes influenced by different compression factors (c=[8,6,4]) at two sweep rates: s=1 oct/min, on the left, and s=4 oct/min, on the right

3. Experimental coupling analysis of structural models

The current research activities are focused on the derivation of numerical and experimental structural test specimen models representing the third major part of the virtual shaker testing simulation environment. The main questions are related to the dynamical coupling between the structural test models and the shaker model, and the coupling between different dynamical substructures of the test specimen and hardware included in the test. The latter is part of this section. Especially, it is of interest to derive experimental and numerical models of the shaker HE, a beam test structure and the coupled system as shown by the pictures in Fig. 6.

The shaker HE is a structural component which is usually used in vibration testing to enlarge the mounting interface between the shaker table and the real test specimen to maximize the versatility of the testing facility. Fig. 6 shows at the top left part a picture of the HE for impact testing equipped with multiple acceleration sensors. Nine one-axial acceleration sensors sensitive in z-direction (orthogonal to the HE surface) are mounted on the frame of the HE and five tri-axial

acceleration sensors are glued closely to the mounting positions (indicated with CP for connection points) of the intended beam test structure.

The beam test structure and its acceleration sensor instrumentation are shown by the bottom left picture of Fig. 6. The advantage of the beam structure is that it can be numerically approximated by a clamped beam to derive a first systems insight and determine modal parameter prior to the test. Additionally, the beam presents a test structure with a high flexibility which is intended to be used later on to verify the control performance in a closed-loop shaker control application. The beam is equipped with four miniature tri-axial acceleration sensors and five tri-axial connection point acceleration sensors mounted on the bottom of the base plate (not shown in the picture) which correspond to the intended mounting positions CP on the HE. The beam's four lightweight miniature accelerometers are selected to avoid any mass loading effect induced to the flexible beam's dynamics. Pictures of the coupled beam structure and HE system are presented on the right part of Fig. 6 whereas the sensor instrumentation is kept unchanged.

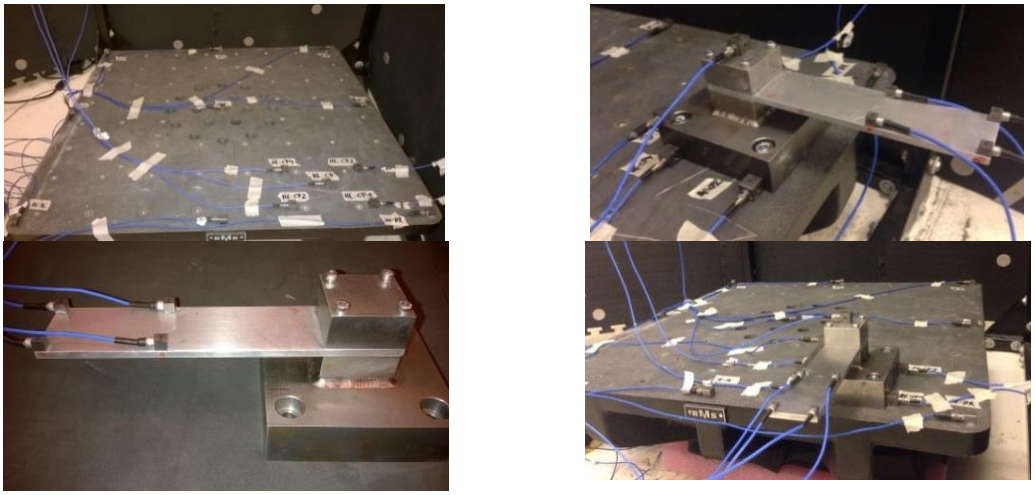

Fig. 6 Pictures of the structural components of the HE at the top left, beam test structure at the bottom left and coupled system on the right, equipped with acceleration sensors for experimental modal analysis, picture courtesy Siemens Industry Software NV

Through a modal analysis survey, the dynamics of the two structures are identified, both separately and in coupled condition. Free-free boundary conditions are considered. The objective is to derive the structural model dynamics and to review the methodologies as well as the preliminary guidelines useful to couple the two structures included in the simulation model. Therefore, the HE and the coupled HE and beam test structure are suspended by foam to simulate free-free boundary conditions during impact testing with excitations at all sensor locations, including HE and connection point sensors. The beam test structure is hung by a flexible cord from a frame during test and is excited especially along the beam and connection points at the base structure with hammer impacts. Some major results of the modal analysis campaign are shortly summarized hereafter whereas a more detailed view on the experimental test results is presented in Waimer *et al.* (2016b). Fig. 7 shows the first and most distinctive mode shapes of the HE on the left, beam test structure in the centre and coupled system on the right estimated from the acquired

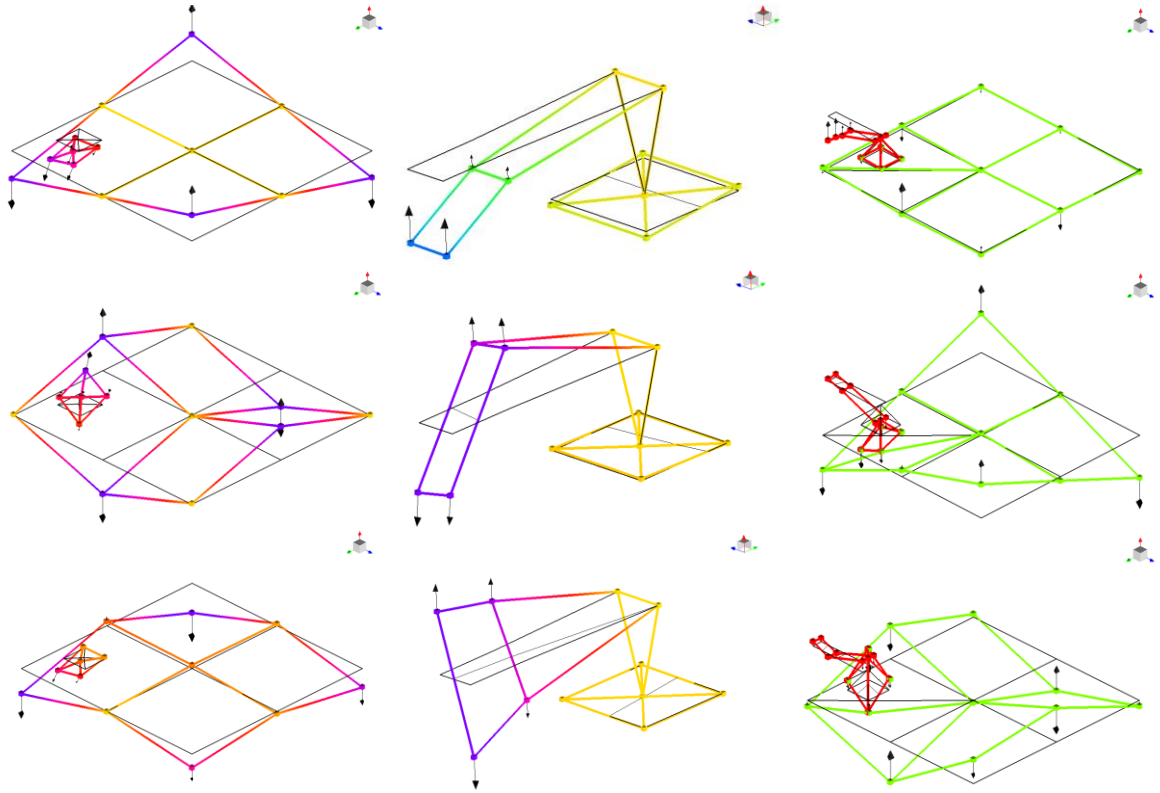

(a) 904.3 Hz, Saddle mode 1192.6 Hz, 1st bending mode 1547.3 Hz, Umbrella mode

(b) 185.8 Hz, 1st bending mode 1009.2 Hz, 2nd bending mode 1148.4 Hz, 1st torsional mode

(c) 155.2 Hz, 1st beam bending 842.1 Hz, HE saddle mode 1135.1 Hz, coupled HE and 2nd beam bending

Fig. 7 First representative modes shapes of the shaker HE (a), beam test structure (b) and coupled HE and beam test structure system (c) in free-free boundary conditions in ascending order from top to bottom

FRFs. As main results the following statements are drawn based on the experimental analyses:

• The beam's 1st bending mode is reduced from the uncoupled case of 185.8 Hz to the coupled case of 155.2 Hz. Additionally, the damping is increased from 2.06% to 4.89%.

• Higher order beam modes are difficult to distinguish since, there is a strong coupling between the modes and the mode shapes are dominated by the HE's eigenvectors.

• The saddle mode of the HE is decreased from 904.3 Hz to 842.1 Hz. The damping is also increased from 0.11% to 0.16%.

• The 1st bending mode of the HE is decreased from 1192.6 Hz to 1135.1 Hz. The damping is also increased from 0.11% to 0.27%.

For all other modes a similar characteristic is observable: the frequency of the modes of the coupled system is decreased whereas the damping is (slightly) increased.

In the future, it is intended to use theoretical techniques as summarized by De Klerk *et al.* (2008) to couple numerical and or experimental subcomponents by methods relying on measured FRFs directly or on a set of identified modes. The experimental campaign described in this section targeted the latter method, where the response of the assembled system is obtained from the modal

model identified on the two subcomponents tested in free-free conditions. This is an important step in the modelling of the vibration test to verify and simulate interactions between the test specimen and shaker testing facility while testing.

4. Dynamical model derivation and sine control prediction

Taking advantage of the availability of experimentally measured FRFs of the coupled HE and beam test structure system, some preliminary analyses to numerically predict the outcome of a sine control vibration test are performed. As the coupling algorithm to connect the different structural subcomponents with each other and with the shaker model is still being investigated, the derived sine controller model is at this stage directly coupled with the acquired FRFs during modal analysis neglecting the shaker dynamics. This introduces the assumption that the sine controller output voltage (shaker drive signal) is defined to be proportional to the shaker current driving the coil of the electromagnetic shaker and the induced force. In practice, this assumption is not valid and, secondly, neglecting the entire shaker dynamics introduces deviations accordingly. However, this preliminary experimentally data driven approach offers the possibility to qualitatively predict responses, spectra and system behaviour as it can be expected in a real test (simulation). Hence, the approach is applied to determine first qualitative numerical test predictions.

The simulations are performed considering the FRFs between the HE centred sensor HE:C and the connection point sensor HE:CP1, and for the coupled case the beam accelerometer B:T1 mounted at the tip of the beam structure, respectively. The impact is chosen to be at HE:C to assume a centred excitation at the HE approximating real test conditions. In principle the modelling and sine control prediction is realised by two basic system identification and simulation approaches.

The first approach presents a direct data driven method by using experimental and/or synthesised FRFs in a look-up-table (LUT) simulation comprising frequency and complex FRF values. While simulating, the correct complex FRF values according to the sweep frequency are selected by applying an interpolation between the sine control sweep frequency and the frequencies in the LUT. To improve the quality of the calculations, the measured FRFs are synthesized by using Polymax, Peeters *et al.* (2004), to derive the modal decomposition linear transfer function model matrix $\boldsymbol{H}(s) \in \mathbb{C}^{N_0 x N_i}$ in Laplace domain $s = \sigma + i\omega$ (also called: pole-residue model),

$$\boldsymbol{H}(s) = \frac{\boldsymbol{x}(s)}{\boldsymbol{F}(s)} = \frac{LR}{s^2} + \sum_{i=1}^{n} \frac{\boldsymbol{\psi}_i \cdot \boldsymbol{l}_i^T}{s - \lambda_i} + \frac{\boldsymbol{\psi}_i^* \cdot \boldsymbol{l}_i^H}{s - \lambda_i^*} + UR \tag{1}$$

with number of outputs N_0 and inputs N_i, n complex conjugated $\bullet^*$ mode pairs λ_i,

$$\lambda_i, \lambda_i^* = -\xi_i \omega_i \pm i\omega_i \sqrt{1 - \xi_i^2} \tag{2}$$

with the undamped natural frequencies ω_i and damping ratios ξ_i, mode shapes $\boldsymbol{\psi}_i \in \mathbb{C}^{N_0 \times 1}$, modal participation factors $\boldsymbol{l}_i \in \mathbb{C}^{N_i \times 1}$, and lower and upper residuals $LR, UR \in \mathbb{R}^{N_0 x N_i}$ to consider the influence of out-of-band modes in the observed frequency range. For the sine control prediction the general Multiple-Input Multiple-Output (MIMO) transfer function matrix of Eq. (1) is reduced to a Single-Input Single-Output (SISO) case, since only HE:C is considered as input and HE:CP1 and B:T1 as outputs separately in two simulations. Consequently, the model is

derived to be capable of calculating much smoother FRFs with a flexible frequency resolution and implemented with the corresponding frequency and complex amplitude values in a synthesised LUT.

Furthermore, the data driven approach is enhanced to derive polynomial z-domain transfer function models,

$$H(z) = \frac{x(z)}{F(z)} = \frac{b_o + b_1 z^{-1} + \ \ldots + b_{2n} z^{-2n}}{1 + a_1 z^{-1} + \ \ldots + a_{2n} z^{-2n}} \tag{3}$$

and linear discrete state-space models,

$$\begin{aligned} \boldsymbol{x}_{k+1} &= \boldsymbol{A}\boldsymbol{x}_k + \boldsymbol{B}\boldsymbol{f}_k \\ \boldsymbol{y}_k &= \boldsymbol{C}\boldsymbol{x}_k + \boldsymbol{D}\boldsymbol{f}_k \end{aligned} \tag{4}$$

with the state/system matrix $\boldsymbol{A} \in \mathbb{R}^{2nx2n}$, input matrix $\boldsymbol{B} \in \mathbb{R}^{2nx1}$, output/observer matrix $\boldsymbol{C} \in \mathbb{R}^{1x2n}$, feedthrough matrix $\boldsymbol{D} \in \mathbb{R}^{1x1}$, state vector $\boldsymbol{x}_k \in \mathbb{R}^{2nx1}$, the input force $\boldsymbol{f}_k \in \mathbb{R}^{2nx1}$ and the system's output $\boldsymbol{y}_k$, from the estimated continuous SISO Polymax model based on Eq. (1).

The discretization of the continuous dynamic model of Eq. (1) is essential for the usage of the LMS Sine Control application in MATLAB®/Simulink®. The closed-loop simulation requires discrete models hence the continuous Polymax model cannot be applied directly in the sine control prediction. Consequently, the derived discrete-time dynamic system models of Eqs. (3) and (4) are directly used in the simulation loop replacing the LUT approach and simultaneously neglecting the need of an interpolation algorithm in the simulation. It is also obvious that the accuracy and correlation of the discretized models with respect to the measured models relies on the quality of the Polymax estimation and the parameters used for the discretization, e.g., sampling times/frequencies and conversion methods such as zero order hold, triangle approximation, impulse variant or bilinear discretization, Cauberghe (2004).

The FRFs used in the simulation are shown on the left of Fig. 8. The measured FRFs of the HE in blue, the measured FRFs of the coupled system in green and the corresponding synthesized FRFs as dashed red and magenta curves. The derived discrete dynamical model representations, z-domain transfer function and discrete state-space model, are shown by the dotted black FRFs and are equal to the synthesized s-domain transfer function model in dashed magenta. Here it is clear that in the coupled configuration the HE's umbrella and 1st bending modes are decreased and more excited than in the uncoupled case. Additionally, the beam's first bending modes in coupled conditions occur in the measured (green) and synthesised (dashed magenta) FRFs. The sine control simulation results with a control reference spectrum of 1 g over the entire frequency range of 10 to 1200 Hz applying a frequency sweep rate of 1 Hz/s is presented on the right of Fig. 8.

The figure on the right shows the acceleration spectra for both cases: coupled HE and beam structure in green using the measured FRFs and in magenta applying the synthesized FRFs, and the HE separately using the synthesized FRF in blue.

The results by using the synthesized FRFs (spectra in magenta) show much smoother and clearer predictions than the measured FRFs (spectra in green) by applying the direct data driven approach using the LUT. This is influenced by the coarse frequency resolution of 4 Hz of the measured FRF in combination with the interpolation and the frequency sweep rate. Consequently, the synthesized FRFs result in a smoother control since the frequency resolution of the FRF can be chosen arbitrarily and adapted to the sine control parameter, and no noise occurs. Despite this improvement, a deviation is also observed at the anti-resonance around 900 Hz. This is a result of the modal parameter estimation and the resulting models (magenta and dotted black) which do not

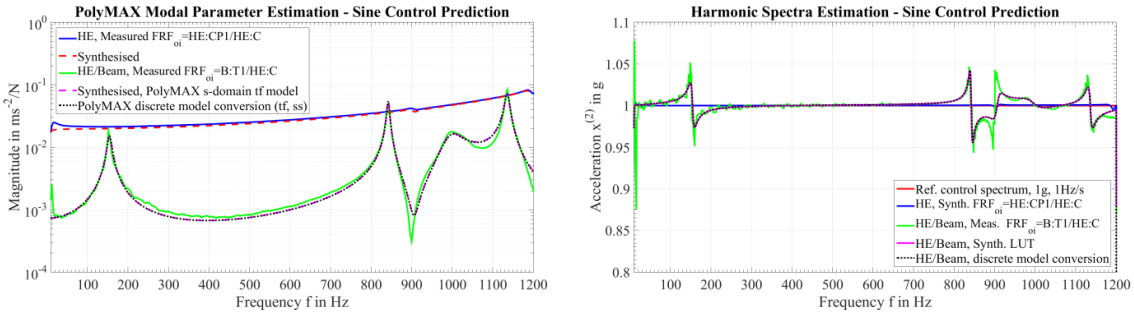

Fig. 8 On the left, experimental/synthesized FRFs for data driven simulation of HE and HE/beam structure coupled models in free-free boundary conditions. On the right, acceleration spectra for preliminary sine control prediction using the estimated models from the left

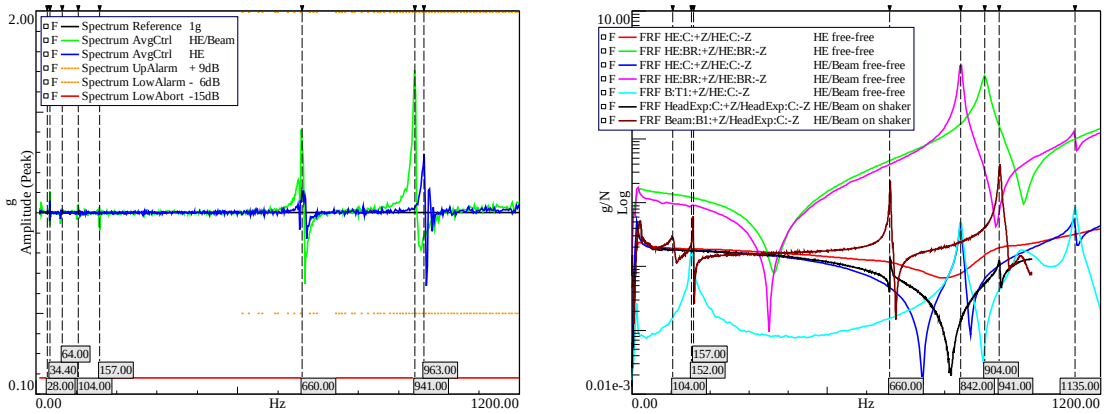

Fig. 9 On the left, real sine control test results with the HE and the coupled HE and test structure model on the shaker. On the right, summary of impact testing FRFs for all configurations: HE and coupled system in free-free and mounted on the HE. Note: different sensor configurations

fully approximate the measured FRF (green) on the left of Fig. 8. Following that, the resulting and predicted acceleration control spectra show this effect as a deviation in the control performance. The simulation results based on the dynamical models in z-domain transfer function and discrete state-space representation derived from the estimated s-domain Polymax model are equal to each other and show the same dynamic results as the data driven approach by using the synthesized LUT approach. All sine control predictions overlap and exhibit an equal characteristic. Consequently, it is summarized for this application and with the given settings, that both modelling approaches, either direct data driven LUT or the dynamic model approach are capable of generating a preliminary reliable sine control prediction. The deviations occurring at the anti-resonance are still being investigated but can be minimized by adapting the modal parameter estimation. The numerical predictions of Fig. 8 are compared to previous experimental sine control test results as given by the left plot of Fig. 9. It needs to be mentioned that the sensor configuration and setup was different compared to the experimental tests introduced in Sec. 3 and used in the simulations of Fig. 8. The main differences in the configurations are the different boundary conditions, that the beam test structure is mounted on a slightly more off-centred position and the not considered interaction between test structure models and shaker dynamics in the numerical

calculations. Additionally, different control sensors were selected. Those are the main reasons why the high frequency modes of the simulations in Fig. 8 differ from the measured modes as shown in Fig. 9.

Nevertheless, the comparison between the numerically simulated and predicted data to the real physical test results is used to draw some preliminary observations. In contrast, it is clearly seen that the 1st bending mode of the beam (approx. 152-157 Hz) is not or only slightly affected by testing the coupled system in free-free or mounted on the shaker table.

In general, it is experimentally observed that an additional mass loading on the HE and the different boundary conditions changes its resonant frequencies significantly and adds new modes comprising coupled test specimen and shaker dynamics. To highlight the importance of the dynamical coupling between the structural models and shaker dynamics in future analysis and simulation environments, the right plot of Fig. 9 shows FRFs acquired during impact testing. Consequently, this summary explains the effects and differences which have been observed by comparing the numerical sine control predictions in Fig. 8 and the real physical test results in Fig. 9, if the coupled test specimen system is in free-free boundary conditions (blue, magenta and cyan curves) or fixed-free clamped to the shaker table (black and brown curves). The 1st beam bending mode clearly occurs if beam structure sensors are considered (cyan and brown curves) but also affects sensors on the HE (magenta). This interaction will increase if heavier test specimens are tested. Additionally, a shaker table rotational (rocking) mode is excited during impact testing at approx. 104 Hz and occurs in the brown FRF prior to the 1st beam bending mode on the right, as well as control deviation in the sine control spectrum on the left of Fig. 9.

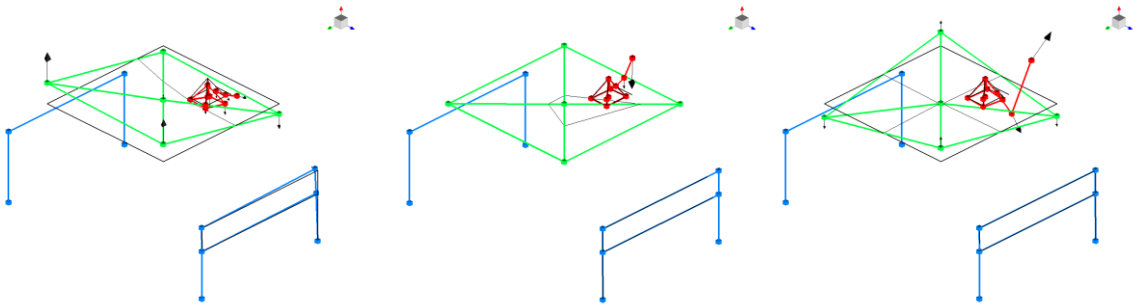

Fig. 10 Shaker sine control test mode shapes with coupled HE and beam structure model (Note: different sensor configuration). On the left, shaker table rocking mode at 34 Hz. In the centre, 1st beam bending mode at 157 Hz of the coupled system. On the right, HE saddle mode at 941 Hz

The acquired test results from sine control and impact testing as shown in Fig. 9 are further used to calculate representative modes shapes of the coupled HE, beam test structure and shaker system. Some of the derived mode shapes are shown in Fig. 10 and are used to interpret the not yet observed control deviations persistent in Fig. 9 on the left. Additionally, to the already detected rotational shaker table mode at 104 Hz, another lower frequency rotational shaker table mode has been detected at 34 Hz which is illustrated by the left mode shape of Fig. 10. The centered mode shape shows the 1st beam bending mode at 157 Hz. The saddle mode of the coupled test structure and shaker system is presented by the right mode shape at approx. 941 Hz (comparison: saddle mode of coupled system in free-free at approx. 842 Hz see Fig. 7, note: different test structure mounting position and different sensor configuration). Additionally, to the mode shapes shown in

Fig. 10 a rotational in-plane shaker table mode is detected at approx. 64 Hz and another higher order rocking mode at 660 Hz. Those mode shapes result in the control deviations which are shown in the sine control acceleration spectrum on the left of Fig. 9. This analysis clearly highlights the necessity to include a coupled structural dynamical test specimen and shaker model in the numerical test prediction to avoid any misinterpretations of measured system characteristics. Additionally, it clarifies how different sensor configurations and setups of assembled test structures may influence the entire system dynamics.

5. Preliminary numerical control performance enhancement

The main focus within this part of the paper is to investigate possible preliminary modifications which can be easily implemented in the numerical and experimental simulation control chain to enhance the control performance. The idea is to use and apply knowledge from the system identification step in terms of FRFs measured and observed prior to the sine control execution, e.g. results from the system self-check to minimize deviations and overshooting especially at resonances occurring in the control spectra (see Figs. 8 on the right and 9 on the left). Basically, it is intended to pre-shape the shaker drives which are equal to the output voltage of the sine controller by pre-multiplication with the inverse FRFs estimated and calculated during the self-check phase. Therefore, the estimated and derived z-domain transfer function model of Sec. 4 is used as system model and is excited in two steps to investigate the effect of adding the drive pre-shaping methodology to the sine control loop.

At first, an open-loop random test is performed to numerically simulate the self-check phase and to calculate the required system FRF from the simulation results, input voltage and output acceleration time series. Subsequently, the inverse of the calculated FRF is implemented in a LUT approach similar to the direct data driven approach in Sec. 4 and used to pre-shape the sine controller output voltage driving the system model within the main sine control prediction. During the sine control simulation, the correct complex inverse FRF values are again selected by applying an interpolation between the sine control sweep frequency and the frequencies in the LUT.

The results are shown by the graphs in Fig. 11. The top left plot shows the pole-zero map of the estimated z-domain discrete polynomial model; poles are indicated as ‘x’ and zeros as ‘o’. The plot confirms the stability of the system since all system poles are within the unit circle. Simultaneously, it is obvious that for the inverse of the system the poles are taking the places of the zeros and vice versa. This causes the poles of the inverse system to be located outside of the unit circle for this SISO case and results in a not stable control for using the inverse system transfer function for pre-shaping the drives. Hence, the LUT approach is applied to overcome the dynamic modelling and simulation instabilities to be capable of pre-shaping the drives with the complex FRF values of the inverse system. The bottom left plot displays the FRFs used for the simulations:

- the z-domain transfer function is shown as dotted black line and used as system model for the open-loop random and closed-loop sine control simulations,
- the magenta and blue coloured FRFs are estimated from open-loop random testing time data with two different simulation times (10 s and 100 s) and two different frequency resolutions (0.5 Hz and 0.05 Hz) and
- the green and dotted red FRFs indicated as theoretical models are directly calculated from the input z-domain model in dotted black. The curves consist of the same different frequency

resolutions (0.5 Hz and 0.05 Hz), as used for the open-loop random FRFs to neglect the possible influence of the open-loop system identification with respect to the pre-shaping algorithm but still being able to analyse the effect of how the frequency resolution affects the accuracy if theoretical models are applied.

The following sine control simulation results with a control reference spectrum of 1 g over the entire frequency range of 10 to 1200 Hz applying a frequency sweep rate of 1 Hz/s are presented at the top right of Fig. 11, and the results considering a fast sweep rate of 10 Hz/s at the bottom right.

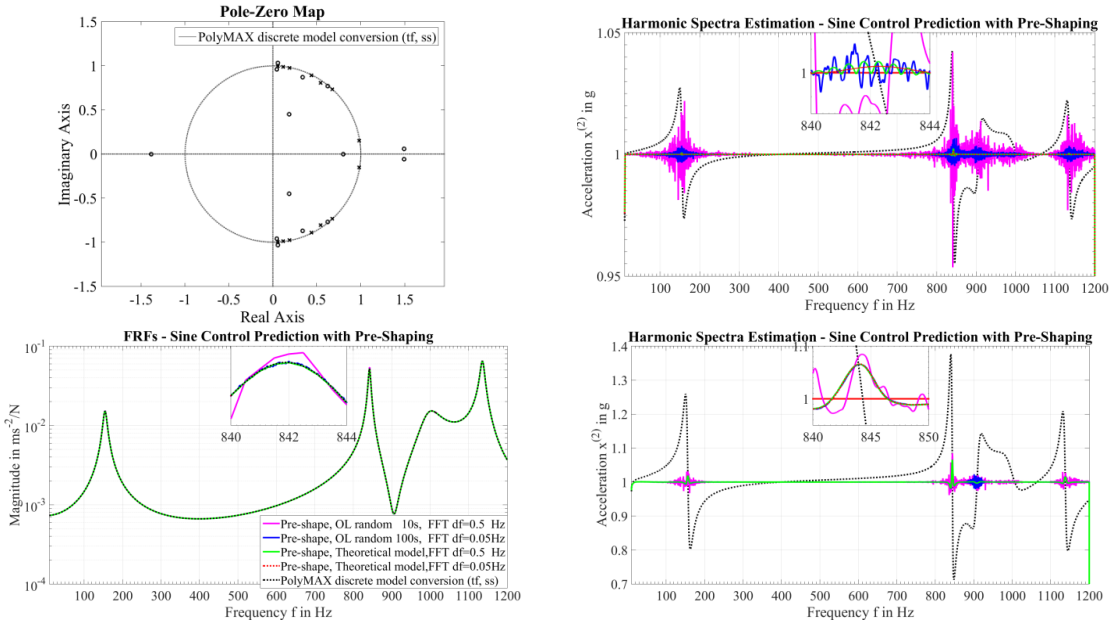

Fig. 11 At the top left, pole-zero map of the derived discrete z-domain polynomial transfer function model. At the bottom left, theoretical and estimated FRFs used for pre-shaping the drives. On the right, sine control predictions with pre-shaping (1 g, 10-1200 Hz) considering a low sweep rate s=1 Hz/s at the top and a high sweep rate s=10 Hz/s at the bottom

For both spectra the pre-shaping methodology is applied. As reference case, the black results can be seen which are calculated without any pre-shaping and clearly exhibit the deviations at the resonances which are intended to be minimized by the pre-shaping algorithm. From a control perspective the overshoots at the system's resonances increase with increasing sweep rate. By applying the inverse values of the calculated FRFs (shown at the bottom left of Fig. 11) for pre-shaping, the deviations occurring in the control spectra are minimized. The calculations indicate that with pre-shaping and higher frequency resolution (0.05 Hz in blue) used in the inverse FRF LUT the control error diminish but, on the contrary, an undesired amount of additional noise is introduced. This added noise is especially obvious in the top right plot calculated by using the slow sweep rate of 1 Hz/s. This is mainly caused by the slight differences in the obtained and used FRFs, in terms of complex amplitude values and changing frequency resolutions (0.05 Hz in blue less noisy and less deviation than 0.5 Hz in magenta), by the interaction with the interpolation used in the LUT and by the handling of small numerical control deviations while simulating.

Consequently, it affects more the results considering the slow sweep rate, dealing with smaller deviations as reported above than the results with the high sweep rate of 10 Hz/s at the bottom right. For both cases, slow and high sweep rate, it is obvious that by increasing the frequency resolution the deviation and noise contribution is minimised and consequently, the control spectra are getting closer to the reference profile. In general, it is observed that the best results, in terms of control deviation and noise contribution, are obtained with using the theoretical models and the lowest frequency resolution of 0.05 Hz. The results of the high sweep rate at the bottom right show already a significant improvement with less noise contribution and clearer spectra for the frequency resolution of 0.5 Hz for both cases; open loop random and theoretical FRFs. This analysis shows how the pre-shaping approach can be applied and indicates its sensitivity with reference to the required frequency resolution to present an alternative for control performance enhancement.

6. Summary and conclusions

The paper reviews the work of the modelling and derivation of an enhanced electrodynamic shaker model based on experimental results and the coupling to a dedicated sine vibration controller in the first part of the paper. In first numerical investigations, the derived coupled shaker to controller model is used to simulate possible challenges which can usually occur during S/C vibration testing of large S/C with not negligible misalignments between CoGs, e.g., beating phenomena. Furthermore, the paper concludes experimental test data and modal analysis results of the shaker HE and a dedicated beam test structure, both in uncoupled and coupled configuration under free-free boundary conditions. Consequently, the experimentally estimated models are numerically coupled to the sine controller model neglecting the shaker model to calculate first numerical sine control test predictions. The calculations are qualitatively evaluated against physical test data of a different test campaign with a diverse sensor setup and boundary conditions, e.g., free-free to fix-clamped interface and the dynamical interaction between test facility, controller and test specimen models. In the last part, the pre-shaping of shaker drives by applying dynamic system knowledge, e.g., gathered during the sine control self-check phase, is numerically analyzed and results in minimized control deviations with respect to the reference profile at the system's resonances.

In the future, it is intended to use this kind of results to derive methodologies to couple experimentally derived structural models and to use them in further numerical closed-loop simulation analyses comprising the electrodynamic shaker and sine controller model. The objective is to derive clear guidelines to successfully develop and execute virtual vibration control tests and to identify the advantages that this process can bring in de-risking test execution and successfully achieve product certification.

Acknowledgments

The authors of this work gratefully acknowledge the European Space Agency under the Network/Partnering Initiative PhD programme (contract No. 4000110039/14/NL/PA) in collaboration with Siemens Industry Software NV and Vrije Universiteit Brussel. A special thank you to Alessandro Cozzani, Matteo Appolloni and Steffen Scharfenberg from ESTEC for their

support and discussions.

References

Appolloni, M. and Cozzani, A. (2007), "Virtual testing simulation tool for the new quad head expander electrodynamic shaker", *Proceedings of the 6th International Symposium on Environmental Testing for Space Programmes*, ESA-ESTEC, Noordwijk, The Netherlands, June.

Appolloni, M., Bureo Dacal, R., Cozzani, A., Knockaert, R. and Thoen, B. (2015), "Multi-degree-of-freedom vibration platform with MIMO controller for future spacecraft testing: and application case for virtual shaker testing", *Proceedings of the 29th Aerospace Testing Seminar (ATS)*, Los Angeles, U.S.A., October.

Bettacchioli, A. (2014), "Simulation of satellite vibration test", *Proceedings of the 13th European Conference on Spacecraft Structure, Materials and Environmental Testing (ECSSMET)*, Brunswick, Germany, April.

Bettacchioli, A. and Nali, P. (2015), "Common issues in S/C sine vibration testing and a methodology to predict the sine test responses from very low-level run", *Proceedings of the 29th Aerospace Testing Seminar (ATS)*, Los Angeles, U.S.A., October.

Cauberghe, B. (2004), "Applied frequency-domain system identification in the field of experimental and operational modal analysis", Ph.D. Dissertation, Vrije Universiteit Brussel, Brussels.

De Klerk, D., Rixen, D.J. and Voormeeren, S.N. (2008), "General framework for dynamic substructuring: History, review, and classification of techniques", *AIAA J.*, **46**(5), 1169-1181.

ECSS (2013), *Space Engineering, Spacecraft Mechanical Loads Analysis Handbook*, ECSS-E-HB-32-26A, http://ecss.nl/hbs/published-hbs-on-line/active-engineering-handbooks/, European Cooperation for Space Standardization (ECSS), Noordwijk, The Netherlands, February.

Lang, G.F. and Snyder, D. (2001), *Understanding the Physics of Electrodynamic Shaker Performance*, Sound and Vibration, October.

Manzato, S., Bucciarelli, F., Arras, M., Coppotelli, G., Peeters, B. and Carrella, A. (2014), "Validation of a virtual shaker testing approach for improving environmental testing performance", *Proceedings of the 26th International Conference on Noise and Vibration Engineering (ISMA)*, Leuven, Belgium, September.

Mao, Z. (2016), "Statistical modeling of wavelet-transform-based features in structural health monitoring", *Proceedings of the 34th International Modal Analysis Conference (IMAC)*, Orlando, U.S.A., January.

Merry, R.J.E. and Steinbuch, M. (2005), "Wavelet theory and applications", *Literature Study, Eindhoven University of Technology, Department of Mechanical Engineering, Control Systems Technology Group*, Eindhoven, The Netherlands, June.

McConnell, K.G. and Varoto, P.S. (1995), *Vibration Testing: Theory and Practice*, 2nd Edition, John Wiley & Sons, New York, U.S.A.

NASA (2014), *Spacecraft Dynamic Environments Testing*, NASA-HDBK-7008, https://standards.nasa.gov/nasa-developed-standards, National Aeronautics and Space Administration (NASA), Office of the NASA Chief Engineer, NASA Technical Standards Program, June.

Peeters, B., Auweraer, H.V.D., Guillaume, P. and Leuridan, J. (2004), "The PolyMAX frequency-domain method: a new standard for modal parameter estimation?", *Shock Vibr.*, **11**(3-4), 395-409.

Ricci, S., Peeters, B., Fetter, R., Boland, D. and Debille, J. (2009), "Virtual shaker testing for predicting and improving vibration test performance", *Proceedings of the 27th International Modal Analysis Conference (IMAC)*, Orlando, U.S.A., February.

Siemens Industry Software NV (2016a), *LMS Test.Lab Environmental*, www.siemens.com/plm/lms, Leuven, Belgium.

Siemens Industry Software NV (2016b), *LMS SCADAS III Data Acquisition Front-end*, www.siemens.com/plm/lms, Breda, The Netherlands.

Waimer, S., Manzato, S., Peeters, B., Wagner, M. and Guillaume, P. (2015), "Derivation and

implementation of an electrodynamic shaker model for virtual shaker testing based on experimental data", *Proceedings of the 29th Aerospace Testing Seminar (ATS)*, Los Angeles, U.S.A., October.

Waimer, S., Manzato, S., Peeters, B., Wagner, M. and Guillaume P. (2016a), "A multiphysical modelling approach for virtual shaker testing correlated with experimental test results", *Proceedings of the 34th International Modal Analysis Conference (IMAC)*, Orlando, U.S.A., January.

Waimer, S., Manzato, S., Peeters, B., Wagner, M. and Guillaume, P. (2016b), "Modelling and experimental validation of a coupled electrodynamic shaker and test structure simulation model", *Proceedings of the 27th International Conference on Noise and Vibration Engineering (ISMA)*, Leuven, Belgium, September.

CC